ZIBELINE INTERNATIONAL PUBLISHING
ISSN: 2773-6202 (Online)
CODEN: JTIOCC

Journal of Technology & Innovation (JTIN)

DOI: http://doi.org/10.26480/jtin.01.2021.10.12

RESEARCH ARTICLE

EFFECT OF POROSITY ON BEHAVIOURS OF PLATE STRUCTURES

P. Phung-Van* and Toan Khong Trong

Faculty of Civil Engineering, Ho Chi Minh City University of Technology (HUTECH), Ho Chi Minh City, Vietnam
****Corresponding Author Email: pv.phuc86@hutech.edu.vn***

ARTICLE DETAILS

Article History:

Received 15 January 2021
Accepted 19 February 2021
Available online 2 March 2021

ABSTRACT

In this paper, effect of porosity on nonlinear analysis of plate structures is presented. Two porous distributions are considered. Governing equations are expressed by using isogeometric analysis (IGA) and the third-order shear deformation theory (TSDT). With these approaches, it is easy to fulfil the C1-continuity requirement of the plate model. The obtained results demonstrate the significance of porosity volume fraction, porosity distributions and volume fraction exponent on nonlinear analysis of the plate structures.

KEYWORDS

isogeometric analysis (IGA), nonlinear analysis, porosity, plate.

1. INTRODUCTION

For Industry 4.0, new materials in engineering play an important role and have been ordered to scientists for inventing. According to this general trend, porous functionally graded materials (PFGM) by integrating both advantages of functionally graded materials and metallic materials with porosities have increased higher fracture toughness, bonding strength, minimization of stress concentration. With a high demand in engineering design to achieve improved structure performance, study on the PFGM structures has attracted several researchers. Nonlinear free vibration of functionally graded sandwich Timoshenko beams with porosities using Ritz method (Chen et al., 2016a) was investigated. The buckling load of porous circular plates (Mojahedin et al., 2016) was studied. Free vibration analysis of rectangular plates with porosities based on a simple first-order shear deformation theory (FSDT) (Rezaei et al., 2017) was performed. In their results, the governing equations of the system were solved analytically for Lévy-type boundary conditions. Free and forced vibrations of functionally graded (FG) Timoshenko beams with non-uniform porosity distribution using Ritz trial functions were reported by Chen et al. (Chen et al., 2016b). Buckling analysis of a solid circular functionally graded (FG) Love-Kirchhoff plate with porous materials subjected to radial loads was presented by Jabbari et al. (Jabbari et al., 2014). Buckling and post-buckling analyses of porous FG plates resting on Pasternak foundations under thermo-mechanical loads using analytical solutions (Cong et al., 2018) was also reported. At present, literature review show that some papers have been focused to dynamic responses of PFGM plates/beams. In the view of practical applications of porous functionally graded materials, mentioned problem should be addressed to accommodate reference solutions for material and structural design. That motivates us study porous plate structures. Thus, this paper develops nonlinear analysis of plate structures with porosities. Porosity-dependent material properties are incorporated to the modified power law index. Some obtained results can be considered as benchmark results to analyze porous plate structures.

2. THEORITICAL FORMULATIONS

A porous plate with length a, width b and thickness h is considered, as shown in Figure 1. Two porosity distributions including even porosities (PFGM-I) and uneven porosities (PFGM-II) are also considered.

Based on the modified rule of mixture, the material properties of PFGM are defined as:

$$P(z) = P_c\left(V_c - \frac{\xi}{2}\right) + P_m\left(V_m - \frac{\xi}{2}\right) \tag{1}$$

where ξ is porosity volume fraction; V_c and V_m are volume fractions of ceramic and metal defined as:

$$V_m + V_c = 1 \quad , \quad V_c = \left(\frac{1}{2} + \frac{z}{h}\right)^n \tag{2}$$

in which subscript c and m represent ceramic and metal, respectively; and n is volume fraction exponent.

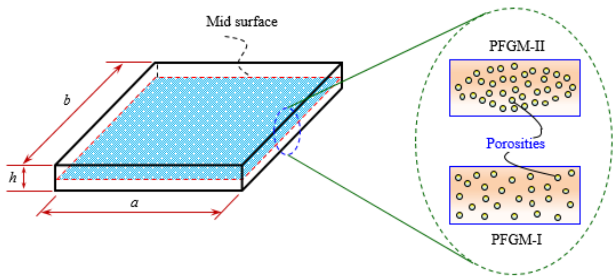

Figure 1: Geometry of FGM nanoplates with two porosity distributions.

Quick Response Code	Access this article online	
	Website: https://jtin.com.my/	**DOI:** 10.26480/jtin.01.2021.10.12

Cite the Article: P. Phung-Van and Toan Khong Trong (2021). Effect of Porosity On Behaviours of Plate Structures. *Journal of Technology & Innovation, 1(1): 10-12.*

Based on the multi-step sequential infiltration technique, material properties of PFGM such as Young's modulus, density, Poisson's ratio, etc., are expressed

$$
\begin{aligned}
&P(z)=\left(P_c-P_m\right)V_c+P_m-\left(P_c+P_m\right)\frac{\xi}{2} \quad \text{for PFGM-I}\\
&P(z)=\left(P_c-P_m\right)V_c+P_m-\left(P_c+P_m\right)\frac{\xi}{2}\left(1-\frac{2|z|}{h}\right) \quad \text{for PFGM-II}
\end{aligned}
\tag{3}
$$

Displacement fields of the plate can be given

$$
\begin{aligned}
&u=u_0+z\beta_x+cz^3\left(\beta_x+w_{0,x}\right)\\
&v=v_0+z\beta_y+cz^3\left(\beta_y+w_{0,y}\right), \quad \left(-h/2\le z\le h/2\right)\\
&w=w_0
\end{aligned}
\tag{4}
$$

where $c = -4/(3h^2)$.

The strains are formulated as follows

$$
\varepsilon_{ij}=\frac{1}{2}\left(\frac{\partial u_i}{\partial x_j}+\frac{\partial u_j}{\partial x_i}\right)+\frac{1}{2}\frac{\partial u_k}{\partial x_i}\frac{\partial u_k}{\partial x_j}
\tag{5}
$$

According to Von Karman theory, the strains in Eq. (5) are rewritten

$$
\begin{aligned}
&\boldsymbol{\varepsilon}=\boldsymbol{\varepsilon}_m+z\boldsymbol{\kappa}_1+z^3\boldsymbol{\kappa}_2\\
&\boldsymbol{\gamma}=\boldsymbol{\varepsilon}_s+z^2\boldsymbol{\kappa}_s
\end{aligned}
\tag{6}
$$

where

$$
\boldsymbol{\varepsilon}_m=\begin{bmatrix}\frac{\partial u_0}{\partial x}\\ \frac{\partial v_0}{\partial x}\\ \frac{\partial u_0}{\partial y}+\frac{\partial v_0}{\partial x}\end{bmatrix}+\frac{1}{2}\begin{bmatrix}\left(\frac{\partial w_0}{\partial x}\right)^2\\ \left(\frac{\partial w_0}{\partial y}\right)^2\\ 2\frac{\partial^2 w_0}{\partial xy}\end{bmatrix}=\boldsymbol{\varepsilon}_L+\boldsymbol{\varepsilon}_{NL};\ \boldsymbol{\kappa}_1=\begin{bmatrix}\frac{\partial \beta_x}{\partial x}\\ \frac{\partial \beta_y}{\partial y}\\ \frac{\partial \beta_x}{\partial y}+\frac{\partial \beta_y}{\partial x}\end{bmatrix};\ \boldsymbol{\kappa}_2=c\begin{bmatrix}\frac{\partial \beta_x}{\partial x}+\frac{\partial^2 w_0}{\partial x^2}\\ \frac{\partial \beta_y}{\partial y}+\frac{\partial^2 w_0}{\partial y^2}\\ \frac{\partial \beta_x}{\partial y}+\frac{\partial \beta_y}{\partial x}+\frac{2\partial^2 w_0}{\partial x\partial y}\end{bmatrix}
\tag{7}
$$

$$
\boldsymbol{\varepsilon}_s=\begin{bmatrix}\beta_x+\frac{\partial w_0}{\partial x}\\ \beta_y+\frac{\partial w_0}{\partial y}\end{bmatrix};\quad \boldsymbol{\kappa}_s=3c\begin{bmatrix}\beta_x+\frac{\partial w_0}{\partial x}\\ \beta_y+\frac{\partial w_0}{\partial y}\end{bmatrix}
\tag{8}
$$

and, $\boldsymbol{\varepsilon}_{NL}$ in Eq. (7) are defined as

$$
\boldsymbol{\varepsilon}_{NL}=\frac{1}{2}\begin{bmatrix}\frac{\partial w_0}{\partial x} & 0 & \frac{\partial w_0}{\partial y}\\ 0 & \frac{\partial w_0}{\partial y} & \frac{\partial w_0}{\partial x}\end{bmatrix}^T\begin{bmatrix}\frac{\partial w_0}{\partial x}\\ \frac{\partial w_0}{\partial y}\end{bmatrix}=\frac{1}{2}\mathbf{A}_\theta\boldsymbol{\theta}
\tag{9}
$$

The stress strain relation is expressed as

$$
\begin{aligned}
&\boldsymbol{\sigma}=\left(\sigma_{xx}\ \ \sigma_{yy}\ \ \sigma_{xy}\right)^T=\mathbf{C}_b\boldsymbol{\varepsilon}=\mathbf{C}_b\left(\boldsymbol{\varepsilon}_m+z\boldsymbol{\kappa}_1+z^3\boldsymbol{\kappa}_2\right)\\
&\boldsymbol{\tau}=\left(\tau_{xz}\ \ \tau_{yz}\right)^T=\mathbf{C}_s\boldsymbol{\gamma}=\mathbf{C}_s\left(\boldsymbol{\varepsilon}_s+z^2\boldsymbol{\kappa}_s\right)
\end{aligned}
\tag{10}
$$

where

$$
\mathbf{C}_b=\frac{E(z)}{1-\nu(z)^2}\begin{bmatrix}1 & \nu(z) & 0\\ \nu(z) & 1 & 0\\ 0 & 0 & \frac{1-\nu(z)}{2}\end{bmatrix};\quad \mathbf{C}_s=\frac{E(z)}{2\left(1+\nu(z)\right)}\begin{bmatrix}1 & 0\\ 0 & 1\end{bmatrix}
\tag{11}
$$

By using isogeometric analysis, displacement fields can be approximated as

$$
\mathbf{u}^h\left(\xi,\eta\right)=\sum_{I=1}^{m\times n}\bar{R}_I\left(\xi,\eta\right)\mathbf{d}_I
\tag{12}
$$

where $\mathbf{d}_I=\left[u_{0I}\ \ v_{0I}\ \ w_{0I}\ \ \beta_{xI}\ \ \beta_{yI}\right]^T$ is degrees of freedom and $\bar{R}_I$ is NURBS basis functions.

The strain can be obtained as

$$
\hat{\boldsymbol{\varepsilon}}=\sum_{I=1}^{m\times n}\left(\mathbf{B}_I^L+\frac{1}{2}\mathbf{B}_I^{NL}\right)\mathbf{d}_I
\tag{13}
$$

where $\mathbf{B}_I^L=\left[\mathbf{B}_I^m\ \mathbf{B}_I^{b1}\ \mathbf{B}_I^{b2}\ \mathbf{B}_I^{s1}\ \mathbf{B}_I^{s2}\right]^T$ is defined

$$
\begin{aligned}
&\mathbf{B}_I^m=\begin{bmatrix}\bar{R}_{I,x} & 0 & 000\\ 0 & \bar{R}_{I,y} & 000\\ \bar{R}_{I,y} & \bar{R}_{I,x} & 000\end{bmatrix},\ \mathbf{B}_I^{b1}=\begin{bmatrix}000 & \bar{R}_{I,x} & 0\\ 000 & 0 & \bar{R}_{I,y}\\ 000 & \bar{R}_{I,y} & \bar{R}_{I,x}\end{bmatrix},\ \mathbf{B}_I^{b2}=c\begin{bmatrix}00 & \bar{R}_{I,xx} & \bar{R}_{I,x} & 0\\ 00 & \bar{R}_{I,yy} & 0 & \bar{R}_{I,y}\\ 00 & 2\bar{R}_{I,xy} & \bar{R}_{I,y} & \bar{R}_{I,x}\end{bmatrix}\\
&\mathbf{B}_I^{s0}=\begin{bmatrix}00 & \bar{R}_{I,x} & \bar{R}_I & 0\\ 00 & \bar{R}_{I,y} & 0 & \bar{R}_I\end{bmatrix},\quad \mathbf{B}_I^{s1}=3c\begin{bmatrix}00 & \bar{R}_{I,x} & \bar{R}_I & 0\\ 00 & \bar{R}_{I,y} & 0 & \bar{R}_I\end{bmatrix}
\end{aligned}
\tag{14}
$$

and $\mathbf{B}_I^{NL}$ is dependent on displacement field given as

$$
\mathbf{B}_I^{NL}=\begin{bmatrix}\mathbf{A}_\theta\\ \mathbf{0}\end{bmatrix}\mathbf{B}_g \text{ where } \mathbf{B}_g=\begin{bmatrix}0\ 0\ \bar{R}_{I,x}\ 0\ 0\\ 0\ 0\ \bar{R}_{I,y}\ 0\ 0\end{bmatrix}
\tag{15}
$$

Equations for nonlinear analysis of the plate can be obtained:

$$
\mathbf{Kd}=\mathbf{F}
\tag{16}
$$

Where

$$
\mathbf{K}=\int_\Omega\left[(\mathbf{B}^L+\mathbf{B}^{NL})^T\mathbf{D}_{bms}(\mathbf{B}^L+\tfrac{1}{2}\mathbf{B}^{NL})\right]\mathrm{d}\Omega\ ;\ \ \mathbf{F}=\int_\Omega\bar{\mathbf{R}}q_0\mathrm{d}\Omega
\tag{17}
$$

in which

$$
\mathbf{D}_{bms}=\begin{bmatrix}\mathbf{A} & \mathbf{B} & \mathbf{E} & \mathbf{0} & \mathbf{0}\\ \mathbf{B} & \mathbf{E} & \mathbf{F} & \mathbf{0} & \mathbf{0}\\ \mathbf{E} & \mathbf{F} & \mathbf{H} & \mathbf{0} & \mathbf{0}\\ \mathbf{0} & \mathbf{0} & \mathbf{0} & \mathbf{A}_s & \mathbf{B}_s\\ \mathbf{0} & \mathbf{0} & \mathbf{0} & \mathbf{B}_s & \mathbf{F}_s\end{bmatrix}
\tag{18}
$$

Where

$$
\begin{aligned}
&\left(\mathbf{A},\mathbf{B},\mathbf{D},\mathbf{E},\mathbf{F},\mathbf{H}\right)=\int_{-h/2}^{h/2}\left(1,z,z^2,z^3,z^4,z^6\right)\mathbf{C}_b\mathrm{d}z\\
&\left(\mathbf{A}_s,\mathbf{B}_s,\mathbf{F}_s\right)=\int_{-h/2}^{h/2}\left(1,z^2,z^4\right)\mathbf{C}_s\mathrm{d}z
\end{aligned}
\tag{19}
$$

3. Numerical Results

To verify the accuracy of the present method, a porous Al/ZrO_2-2 plate (a = 0.2 and h = 0.01) is investigated. The load parameter P and central deflection $\bar{w}$ are formulated:

$$
\bar{w}=\frac{w}{h}\quad ;\quad P=\frac{q_o a^4}{E_m h^4}
\tag{20}
$$

Figure **2** shows nonlinear deflection of the PFGM plate with $\xi=0$.

Reference solutions were performed by Phung-Van et al. (Phung-Van et al., 2017). It can be found that present results match very well with those in ref. (Phung-Van et al., 2017). Also, from Figure **2**, it can be seen that a little bit differences between the present results and the reference solutions. This is because material properties in this study were formulated by using the mixture rule, while those in the reference solutions using Mori Tanaka.

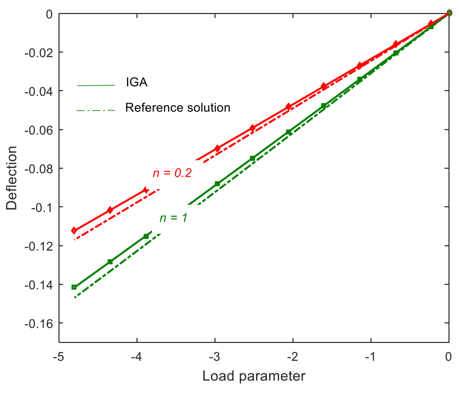

Figure 2: Nonlinear deflection of the PFGM plate made of Al/ZrO_2-2

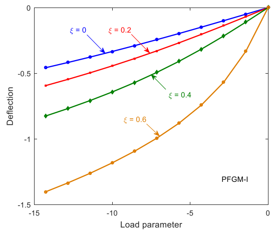

Figure 3: Nonlinear deflection of a SSSS PFGM-I plate made of Al/ZrO_2-2 with *n* = 3.

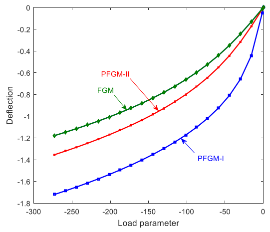

Figure 4: Nonlinear deflection of a CCCC PFGM plate made of Al/Al_2O_3 with *n* = 3, $\xi = 0.3$.

Next, a porous Al/ZrO_2-2 plate (*a* = 10 and *a/h* = 10) with volume fraction *n* = 3 is considered. Effects of porosity parameter on nonlinear analysis of a simply supported PFGM-I plate made of Al/ZrO_2-2 are plotted in Figure 3. It can be observed that with an increase of porous volume fraction leads to a decrease of the stiffness of the plate, nonlinear deflections increase. Comparisons between PFGM-I and PFGM-II plates made of Al/Al_2O_3 (*a* = 10 and *a/h* = 10) are plotted in Figure 4. Deflection of PFGM-II is smaller than that of PFGM-I. So, the stiffness of PFGM-I is smaller than that of PFGM-II.

4. Conclusions

This paper presented effect of porosity on nonlinear bending analysis of plate structures using IGA based on TSDT. The proposed method using NURBS elements naturally fulfils the C^1-continuity requirement of the porous plate. Some benchmark examples for nonlinear responses of the porous plates were investigated. It was obtained that nonlinear behaviors of the plates are influenced by the porous factor. It was also found that porosities reduce the stiffness of the plates and distributions of porosities influence the stiffness significantly.

Acknowledgements

This research is funded by Vietnam National Foundation for Science and Technology Development (NAFOSTED) under grant number 107.02-2019.09.

References

Chen D., Kitipornchai S., Yang J. 2016a. Nonlinear free vibration of shear deformable sandwich beam with a functionally graded porous core. *Thin Wall Struct*. 107:39-48.

Chen D., Yang J., Kitipornchai S. 2016b. Free and forced vibrations of shear deformable functionally graded porous beams. *Int J Mech Sci*. 108:14-22.

Cong P.H., Chien T.M., Khoa N.D., Duc N.D. 2018. Nonlinear thermomechanical buckling and post-buckling response of porous FGM plates using Reddy's HSDT. Aerosp Sci Technol. 77:419-28.

Jabbari M., Mojahedin A., Khorshidvand A.R., Eslami M.R. 2014. Buckling Analysis of a Functionally Graded Thin Circular Plate Made of Saturated Porous Materials. J Eng Mech. 140(2):287-95

Mojahedin A., Jabbari M., Khorshidvand A.R., Eslami M.R. 2016. Buckling analysis of functionally graded circular plates made of saturated porous materials based on higher order shear deformation theory. Thin Wall Struct. 99:83-90.

Phung-Van P., Ferreira A.J.M., Nguyen-Xuan H., Wahab M.A. 2017. An isogeometric approach for size-dependent geometrically nonlinear transient analysis of functionally graded nanoplates. Compos Part B-Eng. 118:125-34.

Rezaei A.S., Saidi A.R., Abrishamdari M., Mohammadi M.H.P. 2017. Natural frequencies of functionally graded plates with porosities via a simple fo ur variable plate theory: An analytical approach. Thin Wall Struct. 120:3 66-77.

Cite the Article: P. Phung-Van and Toan Khong Trong (2021). Effect of Porosity On Behaviours of Plate Structures.
Journal of Technology & Innovation, 1(1): 10-12.